Leiden University Medical Center (LUMC); and is the CEO and has equity in Medis medical imaging systems. Mr. Kitslaar has a research appointment at the LUMC; and is an employee of Medis medical imaging systems. All other authors have reported that they have no relationships relevant to the contents of this paper to disclose. David Bluemke, MD, served as Guest Editor for this paper.

REFERENCES

1. Stone PH, Saito S, Takahashi S, et al. Prediction of progression of coronary artery disease and clinical outcomes using vascular profiling of endothelial shear stress and arterial plaque characteristics: the PREDICTION study. Circulation 2012;126:172–81.

2. Stone GW, Maehara A, Lansky AJ, et al. A prospective natural-history study of coronary atherosclerosis. N Engl J Med 2011;364:226–35.

3. de Graaf MA, Broersen A, Kitslaar PH, et al. Automatic quantification and characterization of coronary atherosclerosis with computed tomography coronary angiography: cross-correlation with intravascular ultrasound virtual histology. Int J Cardiovasc Imaging 2013;29:1177–90.

4. Papadopoulou SL, Neefjes LA, Garcia-Garcia HM, et al. Natural history of coronary atherosclerosis by multislice computed tomography. J Am Coll Cardiol Img 2012;5 Suppl:S28–37.

5. Papadopoulou SL, Neefjes LA, Schaap M, et al. Detection and quantification of coronary atherosclerotic plaque by 64-slice multidetector CT: a systematic head-to-head comparison with intravascular ultrasound. Atherosclerosis 2011; 219:163–70.

Lumen Measurements From Quantitative Coronary Angiography and IVUS: A PROSPECT Substudy

Using multilesion, multivessel, multi-imaging modality data from PROSPECT (Providing Regional Observations to Study Predictors of Events in the Coronary Tree) (1), we examined differences between angiographic and intravascular ultrasound (IVUS) lumen dimension measurements and factors that affected the discrepancy. Baseline grayscale and IVUS virtual histology studies in 3,017 nonculprit lesions (658 patients) were coregistered to the angiographic roadmap by an individual blinded to the IVUS and quantitative coronary angiography (QCA) analyses; IVUS and QCA measurements were performed at separate core laboratories (Cardiovascular Research Foundation, New York, New York) (2). The primary comparison was IVUS versus QCA in-lesion minimal lumen diameter (MLD) using a Passing-Bablok approach with differences between IVUS- and QCA-measured MLD assessed using Kendall's concordance coefficients and Bland-Altman plots. A model with a generalized estimating equation approach was used to compensate for potential cluster effects of multiple lesions in the same patient. IVUS pullback lengths were left anterior descending coronary artery (LAD) 72.9 ± 26.6 mm, left circumflex coronary artery (LCX) 61.2 ± 25.1 mm, and right coronary artery (RCA) 82.9 ± 30.6 mm; distances from the ostia were grouped in tertiles to identify proximal, mid, and distal segments. Statistical analyses, except Passing-Bablok regressions, were conducted using SAS version 9.2 (SAS Institute, Cary, North Carolina); Passing-Bablok analyses were conducted using R version 3.2.1 (R Foundation for Statistical Computing, Vienna, Austria) using the ggplot2 package version 1.0.0 and mcr package version 1.2.1.

There was a strong concordance between IVUS MLD and QCA MLD (Kendall's $W = 0.89$, $p < 0.001$) (**Figure 1A**); however, QCA underestimated MLDs in small vessels and overestimated MLDs in large vessels compared with IVUS. The "intersection MLD" was 3.8 mm, with smaller vessels having an MLD <3.8 mm and larger vessels an MLD >3.8 mm. The Bland-Altman plot of IVUS minus QCA MLD (**Figure 1B**) indicated that QCA underestimated MLD compared with IVUS: mean difference 0.21 ± 0.48 mm and median difference 0.23 mm (interquartile range [IQR]: −0.05 to 0.52]. In lesions with IVUS MLD >QCA MLD, the median difference was 0.39 mm. In lesions with IVUS MLD <QCA MLD, the median difference was −0.26 mm. The overall discrepancy was 16.5 ± 13.9% or a median of 13.1% (IQR: 6.2% to 22.5%).

There was a strong concordance between IVUS versus QCA MLD in the LAD, LCX, and RCA, separately: LAD, QCA MLD 2.55 ± 0.80 mm versus IVUS MLD 2.71 ± 0.60 mm, Kendall's $W = 0.88$, $p < 0.001$; LCX, QCA MLD 2.50 ± 0.73 mm versus IVUS MLD 2.72 ± 0.60 mm, Kendall's $W = 0.89$, $p < 0.001$; and RCA, QCA MLD 2.73 ± 0.70 mm versus IVUS MLD 2.99 ± 0.61 mm, Kendall's $W = 0.88$, $p < 0.001$. There was also a strong concordance in each proximal, middle, and distal subsegment ($p < 0.001$; data not shown); however, the mean discrepancy between IVUS MLD and QCA MLD in the proximal LAD was smaller than the mid or distal LAD (median 0.07 mm [IQR: 0.74 mm], 0.24 mm [IQR: 0.56 mm], 0.30 mm [IQR: 0.52 mm], respectively) or the proximal, mid, or distal LCX (median 0.21 mm [IQR: 0.49 mm], 0.22 mm [IQR: 0.56 mm], 0.21 mm [IQR: 0.54 mm], respectively) or RCA (median 0.22 mm [IQR: 0.61 mm], 0.30 mm [IQR: 0.53 mm], 0.31 mm [IQR: 0.55 mm], respectively) subsegments. Conversely, scatter was greatest in the proximal LAD subsegment (range [min-max MLD difference]): LAD, proximal 3.89 mm (−2.61 to 1.29 mm), mid 3.07 mm (−1.38 to 1.69 mm), distal 3.24 mm (−1.82 to 1.42 mm); LCX, proximal 3.16 mm (−1.40 to 1.75 mm), mid 3.43 mm (−1.14 to 2.29 mm), distal 2.75 mm (−1.41 to 1.34 mm); and RCA, proximal 3.41 mm (−1.47 to 1.94 mm), mid 2.87 mm (−1.28 to 1.59 mm), distal 3.26 mm (−1.60 to 1.66 mm).

An IVUS MLD minus QCA MLD difference >0.23 mm (median) and an IVUS >QCA MLD were associated with longer lesions ($p = 0.001$, $p = 0.0016$,

FIGURE 1 Comparison Between MLDs Measured With IVUS and QCA

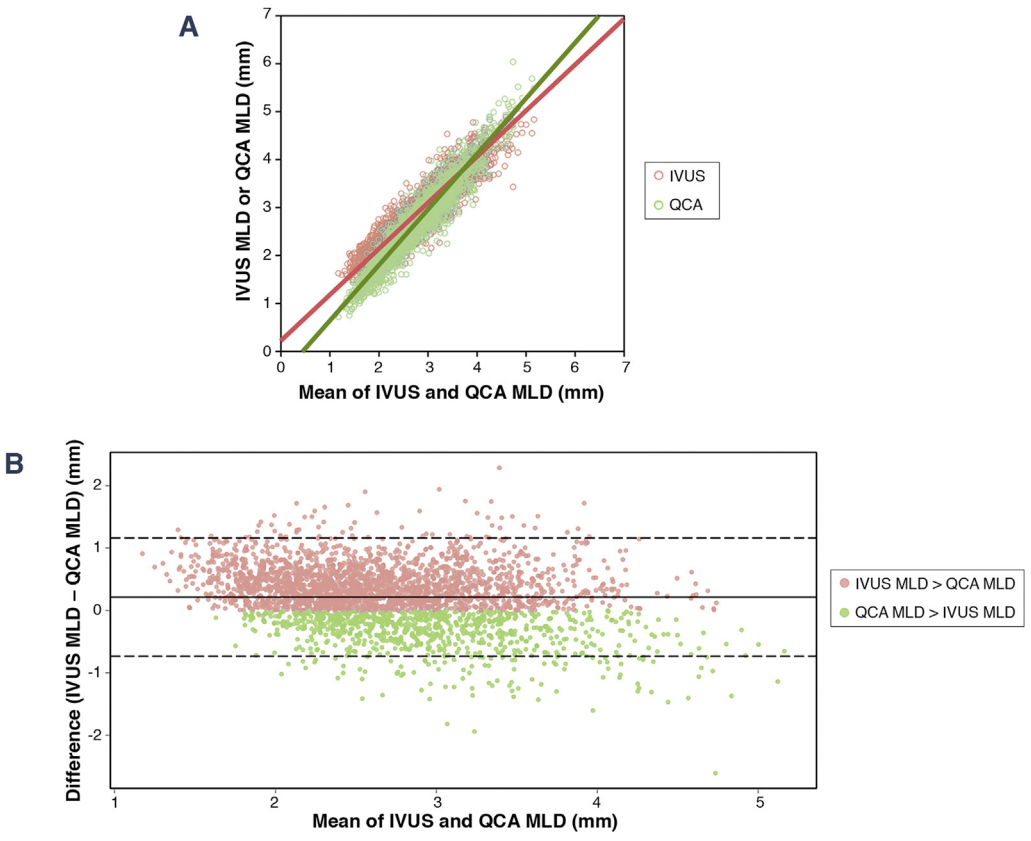

(A) Passing-Bablok regression of minimal lumen diameter (MLD) measured with intravascular ultrasound (IVUS) or quantitative coronary angiography (QCA) versus the mean of the measured with and. Intersection = 3.8 mm. **(B)** Bland-Altman analysis of MLD measured with IVUS versus QCA.

respectively). An IVUS MLD minus QCA MLD difference ≤0.23 mm (median) and IVUS ≤QCA MLD were associated with larger plaque burden ($p = 0.0006$, $p < 0.0001$, respectively) and a larger amount of dense calcium ($p < 0.0001$, $p = 0.0004$, respectively), but also larger reference vessels ($p < 0.0001$, $p < 0.0001$, respectively) with less severe angiographic diameter stenosis ($p < 0.0001$, $p < 0.0001$, respectively). Plaque rupture and necrotic core were predictors of only IVUS MLD minus QCA MLD >0.23 mm and ≤0.23 mm (data not shown).

Only nonculprit lesions in acute coronary syndromes patients were analyzed, and culprit lesions were not included. The size of the IVUS catheter may have contributed to some of the difference between QCA and IVUS.

In conclusion, in small coronary arteries, QCA underestimated lumen diameters compared with IVUS, whereas in large coronary arteries, QCA overestimated lumen diameters compared with IVUS. Among proximal, mid, and distal subsegments of the 3 arteries, the discrepancy between IVUS and QCA MLD was least in the proximal LAD; however, the scatter was greatest.

Kosaku Goto, MD, PhD
Gary S. Mintz, MD
Claire Litherland, MS
Alexandra J. Lansky, MD
Giora Weisz, MD
John A. McPherson, MD
Bernard De Bruyne, MD, PhD
Patrick W. Serruys, MD, PhD
Gregg W. Stone, MD
Akiko Maehara, MD*

*Cardiovascular Research Foundation
111 East 59th Street, 12th Floor
New York, New York 10022
E-mail: amaehara@crf.org

http://dx.doi.org/10.1016/j.jcmg.2015.07.006

Please note: Dr. Mintz is a consultant for Volcano Corporation, Boston Scientific, InfraReDx, and ACIST; has received fellowship/grant support from Volcano Corporation, Boston Scientific, and InfraReDx; and has received honoraria from Boston Scientific, InfraReDx, and ACIST. Dr. Weisz is on the advisory board of Angioslide, AstraZeneca, Calore Medical, Corindus, Medivizor, and Medtronic. Dr. De Bruyne receives grant support and consulting fees to his institution from St. Jude Medical. Dr. Maehara has received grant support from Boston Scientific; is a consultant for Boston Scientific and ACIST; and has received speaker's fees from St. Jude Medical. All other authors have reported that they have no relationships relevant to the contents of this paper to disclose. Sotirios Tsimikas, MD, served as the Guest Editor for this article. (PROSPECT: An Imaging Study in Patients With Unstable Atherosclerotic Lesions; NCT00180466)

REFERENCES

1. Stone GW, Maehara A, Lansky AJ, et al. A prospective natural-history study of coronary atherosclerosis. N Engl J Med 2011;364:226–35.

2. Maehara A, Cristea E, Mintz GS, et al. Definitions and methodology for the grayscale and radiofrequency intravascular ultrasound and coronary angiographic analyses. J Am Coll Cardiol Img 2012;5 Suppl:S1–9.

Calcified Constrictive Pericarditis: Prevalence, Distribution Patterns, and Relationship to the Myocardium

Constrictive pericarditis (CP) represents the final stage of chronic inflammation of the pericardium with impediment of cardiac filling. The morphologic hallmark is a stiff fibrotic, not infrequently calcified, pericardium. Computed tomography (CT) is a better imaging modality to depict the presence and to evaluate the extent of calcifications than traditional methods such as chest x-ray or fluoroscopy. The fibro-calcified process, however, may extend into the underlying myocardium as well and CT has a distinct advantage to identify this. In this retrospective study (2005 to 2015), we present our experience of using CT to identify calcific myocardial penetration in a clinical series of 43 patients (36 men, mean 64 ± 11 years of age) with CP, diagnosed at echocardiography (n = 40), cardiac catheterization (n = 29), or during pericardiectomy (n = 28). CT was performed in 41 patients (95%). Cardiac magnetic resonance was available in 33 patients. No underlying cause for CP was found in the majority (n = 24). History of prior cardiac surgery (n = 6), previous thoracic radiotherapy (n = 4), infections (tuberculosis in 5 and non-tuberculosis in 3), and asbestosis (n = 1) were etiologies in the rest.

Pericardial calcifications were present in 28 of 41 patients (68%) on CT, compared to 21 of 43 patients (49%) at conventional chest x-ray and 14 of 29 patients (48%) at cardiac catheterization. The basal part of the ventricles and atrioventricular grooves were most frequently calcified (left ventricle n = 23, right ventricle n = 20), followed by the right ventricular outflow tract (n = 20), and the right atrium (n = 17). Pericardial calcifications were thickest in the basal parts of the ventricles and atrioventricular grooves (right 4.2 ± 2.3 mm, range 1 to 10 mm; left 3.6 ± 2.0 mm, range 1 to 8 mm).

FIGURE 1 Representative Images of Deep Myocardial Penetration of Calcifications at Computed Tomography and CMR

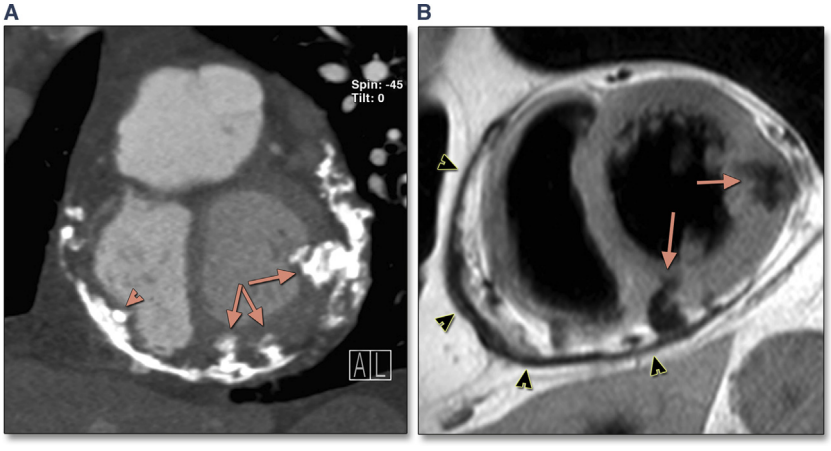

(A) A 61-year-old woman with an idiopathic form of constrictive pericarditis (CP). Presence of massive pericardial calcifications with massive, deep penetration of both left ventricular (LV) **(arrows)** as well as right ventricular wall **(arrowhead)**. **(B)** A 62-year-old man with history of tuberculosis. T1-weighted spin-echo cardiac magnetic resonance (CMR). Irregular thickened pericardium **(black arrowheads)**. The calcifications, appearing hypointense, penetrate deeply the inferior and lateral LV wall **(arrows)**. At cine cardiac magnetic resonance (Online Video 1), the involved segments are thickened and hypocontractile (lateral wall segment end-diastolic wall thickness 17 mm, systolic wall thickening 6%) and the left ventricle shows a mild systolic dysfunction (LV ejection fraction 53%).